Scientific Research Publishing

Materials Sciences and Applications, 2025, 16(6), 307-326
https://www.scirp.org/journal/msa
ISSN Online: 2153-1188
ISSN Print: 2153-117X

Enhancing Mud Brick Sustainability Using Nanomaterials for Restoration Adobe Enclosure of Dendera Temple, Qena, Egypt

Essam H. Mohamed

Archaeological Conservation Department, Faculty of Archaeology, South Valley University, Qena, Egypt
Email: essam.mohamed@arch.svu.edu.eg

How to cite this paper: Mohamed, E.H. (2025) Enhancing Mud Brick Sustainability Using Nanomaterials for Restoration Adobe Enclosure of Dendera Temple, Qena, Egypt. *Materials Sciences and Applications*, **16**, 307-326.
https://doi.org/10.4236/msa.2025.166018

Received: April 5, 2025
Accepted: June 3, 2025
Published: June 6, 2025

Copyright © 2025 by author(s) and Scientific Research Publishing Inc.
This work is licensed under the Creative Commons Attribution International License (CC BY 4.0).
http://creativecommons.org/licenses/by/4.0/

Open Access

Abstract

The adobe enclosure of Dendera temple is one of the most important remaining archaeological clay in ancient Egyptian temples. Field observations indicated significant preservation problems, primarily resulting from swelling caused by water absorption and humidity fluctuations, which compromised the structural and aesthetic integrity of the adobe enclosure of the temple. This study focuses on analyzing the effectiveness of two different classes of nanomaterial (calcium hydroxide ($Ca(OH)_2$) - silicon dioxide (SiO_2)) in resisting swelling, which occurs as a result of the exposure of mud brick to the effects of moisture and salts. To achieve this objective, nanomaterial enhanced mud brick specimens were prepared, and then subjected to artificial weathering experiment ((15) cycles of salt crystallization). A comprehensive analysis was conducted on the deteriorated mud brick specimens using X-ray diffraction for mineralogical analysis, stereomicroscope, polarized light microscope (PLM) and scanning electron microscope (SEM). Nanomaterial enhanced mud brick efficacy was assessed before and after being subjected to the artificial ageing cycles by evaluation of physical properties (bulk density, water absorption, porosity), Atterberg limits test (liquid limit (LL), plastic limit (PL), plasticity index (PI)), examination of the internal structure by SEM and compressive strength resistance. The results of the study showed that adding nanomaterials reduced the ability of clay minerals to interact with water contaminated with salt, as the samples treated with Nano lime recorded a plasticity rate of 27%, with a decrease rate of 40.65% compared to the untreated specimens, and achieved a resistance rate to swelling pressure of 3.6 MPa. The specimens treated with Nano silica recorded a plasticity rate of 26%, with a decrease rate of 42.85% compared to the untreated specimens, and achieved a resistance rate to swelling pressure of 3.8 MPa.

Keywords

Dendera Temple's Adobe Enclosure, Swelling Phenomena, Nanomaterial, The Artificial Ageing

1. Introduction

Mud brick or adobe has been used as building material from the earliest Neolithic structures in ancient monuments in Egypt (Abydos and Hierakonpolis). The oldest known evidence of mud brick production dates to the Middle Pre-dynastic, which falls in the first half of the fourth millennium BC (*i.e.*, Naqada IB to IIIA, and the Chalcolithic in the Near East). Additionally, mud bricks were found lining two tombs in Abydos. Further evidence of mud brick was uncovered in the tombs of the First and Second Dynasties in both Abydos and Saqqara. The use of mud bricks in construction dates back to the Neolithic period, as evidenced by the discovery of mud lumps with organic materials in Merimde Beni-Salame's phase III. Additional examples from the Early to Middle Predynastic period were found in Upper and Lower Egypt [1] [2]. A notable scene depicting the stages of mud brick making is recorded on the walls of the tomb of Vizier Rekhmire in Qurna, dating back to the Eighteenth Dynasty. The scene shows a brick kiln with a hole for collecting water, two men fetching water from it, a place for fermenting clay, men mixing clay with water, men placing it in small piles at the work site, and others engaged in various activities. Mud bricks are composite building materials made up of various natural components, including rock fragments and organic fibers, held together by clay minerals that serve as a binding agent. The widespread and enduring use of mud bricks across different periods can be attributed to the abundance of their primary ingredients, namely soil and water, as well as their cost-effectiveness [3] [4].

One of the challenges with clay-based building materials is their susceptibility to water-induced deterioration, such as capillary absorption and wet-dry cycles. The swelling of clay minerals due to moisture further exacerbates structural weakening, highlighting the need for effective protection and stabilization measures [5] [6]. Swelling occurs when polar molecules, such as water, are absorbed into the interlayer spaces of clay minerals, causing the interplanar distance to expand. This expansion generates internal stresses, which can ultimately lead to adobe material failure [7] [8], expansive clay minerals pose significant challenges due to their complex nature, making it difficult to accurately characterize and predict their behavior. Their swelling is influenced by various environmental factors, including water content, external loads, temperature, salt solutions, interlayer cation species, soil types, and treatment materials. In the preservation of archaeological mud bricks, water is a key factor, as its interaction with expansive clay minerals can cause swelling, disruption, and eventual structural failure [9] [10]. The high risk of severe damage to mud-bricks highlights the necessity of consolidation to re-

store their structural integrity and stabilize the swelling clay minerals, thereby preventing further deterioration of the archaeological material.

The consolidation process is essential for restoring the strength and coherence of deteriorated materials, ensuring they can withstand environmental challenges. Ideal consolidants should demonstrate durability, adequate penetration, controlled porosity modification, and material compatibility. Additionally, coatings applied to porous materials need to be waterproof while allowing vapor transmission, chemically inert, and environmentally stable to protect the material effectively [11]. Nanomaterials are revolutionizing the preservation of cultural heritage by providing effective solutions for strengthening and protecting historical structures, monuments, and relics. These materials are designed to maintain the authenticity of the monumental materials while significantly improving their resilience and longevity [12].

Nanoparticle suspensions of calcium hydroxide are increasingly used in the preservation of historical materials due to their ability to form a durable protective layer through carbonation. As calcium hydroxide converts to calcium carbonate, it creates a consolidated surface that reinforces the underlying material. This method is especially beneficial for mud bricks, given the natural presence of calcium carbonate in their composition. The nanoparticles' small size allows for deep penetration into the material, ensuring a robust and long-lasting treatment [13].

The effectiveness of calcium hydroxide ($Ca(OH)_2$) stems from its short-term and long-term interactions with clay minerals in the presence of water. In the short term, calcium ions facilitate cation exchange, reducing repulsive forces between aluminosilicate layers and promoting flocculation. This process enhances the material's stability by mitigating swelling and shrinkage properties. When water is present, the short-term and long-term interactions with clay phases determine the effective role of $Ca(OH)_2$. When CaO is present in soils, cation exchange is temporarily carried out, which lowers the repulsion forces between the alumino-silicate layers and eventually causes the layers to flocculate, improving the swelling and shrinkage characteristics of the soils [14]. Subsequently, silica and alumina dissolve from the aluminosilicate layers in an alkaline environment (with an excess of OH^-). They then react with Ca^{2+} through the pozzolanic reaction to form cementitious compounds like calcium silicate hydrates (CSH), calcium aluminate hydrates (CAH), and calcium alumino-silicate hydrates (CASH) [15].
Consolidation of mud bricks has made extensive use of silica-based consolidant products, particularly those based on tetra-ethyl-ortho-silicate (TEOS), which significantly reduces the porosity of the material. The preferred consolidants for adobe consolidation are silicic acid esters (SAE), which hydrolyze to produce amorphous silica, which is defined by disordered lattices of tetra-coordinated silica. When there is moisture present, this silica consolidates to create ethyl silicate [16].

In numerous nations where adobe masons were extensively utilized in historic architecture, the issue of conserving and restoring old mud bricks poses a serious threat to the preservation of architectural heritage. So, this study aims to preserve

and protect the mud bricks used in the adobe enclosure of the Dendera Temple from the effects of moisture, represented by groundwater rich in salts. To achieve this, the study methodology is based on an experimental study to examine the effectiveness of two different classes of nanomaterial (calcium hydroxide ($Ca(OH)_2$) and silicon dioxide (SiO_2)) in resisting swelling.

2. The Adobe Enclosure of Dendera Temple

West of Qena city, near the town of Dendera on the Nile River's west bank, stands the Temple of Goddess Hathor. It is located at longitude 32˚40'14.08"N and latitude 26˚8'29.96"E [17] [18]. This temple is surrounded by a huge mud-brick enclosure, measuring approximately 284.5 meters from north to south and approximately 278.21 meters from east to west (**Figure 1**). The courses of the adobe enclosure walls were constructed using the ancient Egyptian technique, and it was discovered via archeological research that this adobe enclosure served two purposes. It served as a fortress to defend the temple's architectural units from adversaries and predatory animals in the first place. The second function was symbolized by settlement, as a collection of chambers and dwellings housing the temple priests were discovered inside this wall.

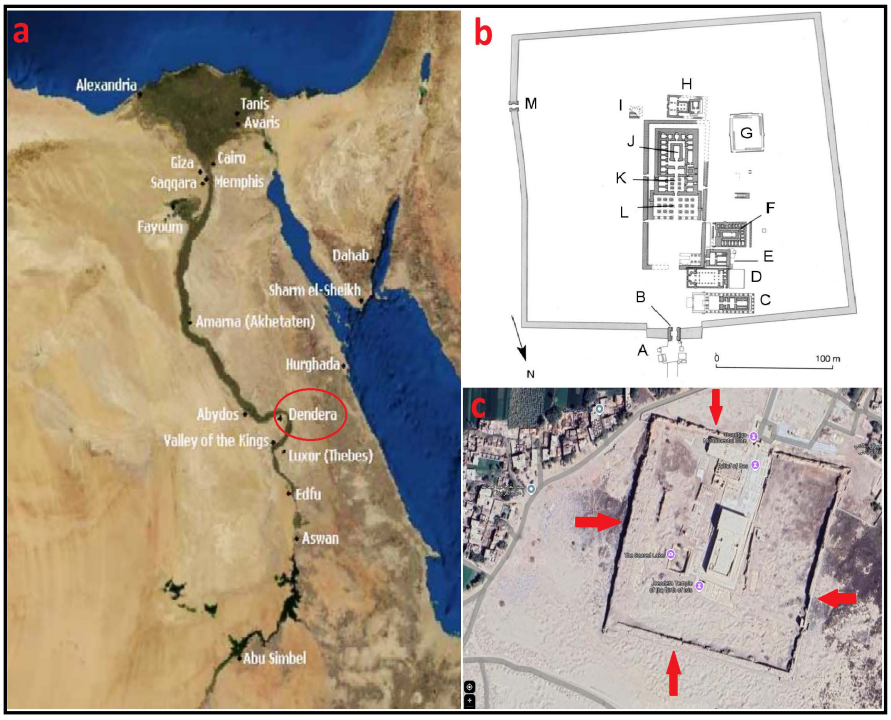

Figure 1. (a) Egypt map, the circle indicates the site of Dendara temple. (b) Plan of Dendara temple and its adobe wall [18]. (c) The site of Dendara temple and its surrounding (Google earth).

The adobe enclosure surrounding the Dendera temple has endured damage from both ancient and modern factors. Historical events such as earthquakes and flash floods have taken their toll, while contemporary threats include agricultural

activities, rising groundwater levels, encroaching urban development, and human-induced destruction. Additionally, pollution and contamination of the groundwater by salts beneath the temple site, along with overgrowth of vegetation, further exacerbate the deterioration.

Variations in groundwater levels, extreme temperatures, and salt contamination of the groundwater beneath the temple have all affected the mud-brick used to construct the adobe enclosure of Dendera Temple. Together, these factors create a complicated deterioration mechanism that degrades the temple's mud brick. Rising temperatures and changes in the relative humidity content of the atmosphere cause the moisture trapped within the material's pores to evaporate. This causes the dissolved salts within the structure to crystallize, causing internal cracks and the loss of cohesion among the material's molecules, causing them to separate from the rest of the structure [19] [20]. Moisture penetration into adobe walls or unprotected surfaces triggers a breakdown in the soil's cohesion and degradation of organic binders like straw, weakening the overall structural stability. When the upper sections of adobe structures lack sufficient protection or the protective measures fail, rainwater infiltrates existing micro-cracks, leading to the deterioration of building materials. The impact of rainwater on the upper walls results in the formation of fissures and cracks. **Figure 2** shows the damage to the mud bricks used in the adobe enclosure of the Dendera Temple.

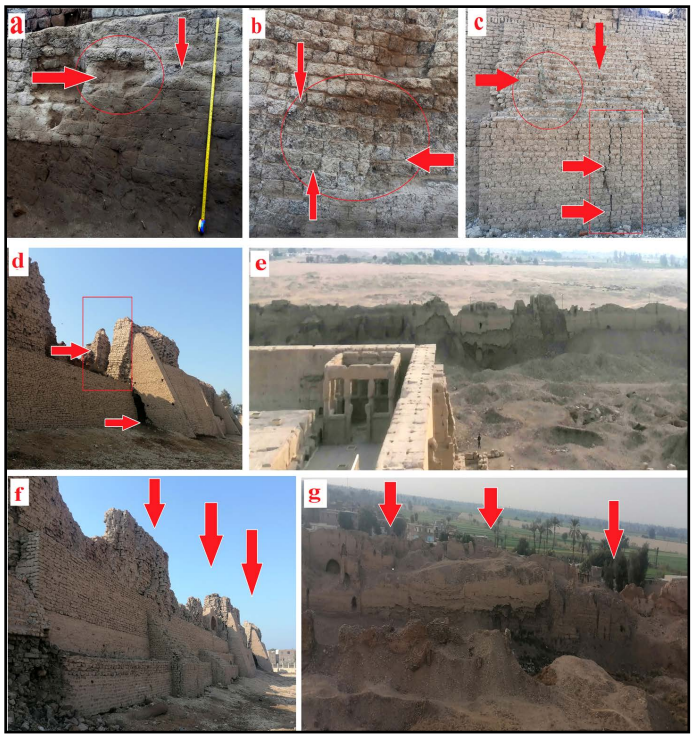

Figure 2. (a) Swelling of brick blocks due to the effect of ground water. (b) Erosion and loss in adobe blocks. (c) Cracks and separation in the mud brick blocks used in the reinforcement process. (d) Separation of the mud brick blocks used in the wall as well as separation of the mud brick blocks used in the reinforcement. (e) The southwestern side of the wall. (f) The northwestern side of the wall.

3. Materials and Methods

3.1. Preparation of the Mud-Brick Specimens

Specimens of adobe bricks were prepared with characterization similar to those of ancient bricks, aiming to study their physical and mechanical properties and compare them to the archaeological bricks. This can help in understanding how to preserve ancient bricks and develop restoration methods. Blocks of mud bricks enhanced with nanomaterial were also prepared and compared with samples that had been prepared with natural materials.

The proposed mud-brick blocks consisted of the following materials:

Essential additives: Soil from the Dendera Temple site was used and mixed with (20% wt) Nile silt. The clay was brought and washed with distilled water several times to get rid of the salts, then it was dried and then ground well in preparation for use.

Secondary additives: They consist of inorganic materials such as lime and pottery powder. Organic additives consist of straw.

Before mixing the components, it was necessary to determine the required water content, which was achieved by conducting a plasticity limit test. This test determines the point at which the mixture becomes plastic.

Nanomaterial additives: Two types of nanomaterial (calcium hydroxide ($Ca(OH)_2$) - silicon dioxide (SiO_2)) were used and added to the components used in preparing the mud brick blocks.

Nano lime was prepared using a magnetic heating stirrer, 10 g of calcium chloride ($CaCl_2$) was mixed with 200 mL of deionized water for 60 minutes to create nano lime. Hydrochloric acid (HCl) at a concentration of 0.1 to 0.5 mL was then gradually added to the first solution while being continuously stirred. After adding 1 gram of sodium hydroxide (NaOH) gradually to the first solution at a 25% concentration, the mixture was swirled for two to four hours at 90˚C in a water bath. Following that, deionized water and alcohol were used to filter and wash the white product until Cl^- was found [21].

A sodium silicate solution was prepared by dissolving 10 grams of sodium silicate in 200 milliliters of deionized water. The mixture was stirred for 30 minutes using a magnetic stirrer with heating. Hydrochloric acid (HCl, 0.1 - 0.5 milliliters) was slowly added to the solution while continuously stirring. Next, 1 gram of 25% ammonia (NH_3) was slowly added to the solution, which was then stirred for 3 hours at 80˚C in a water bath. The resulting white product was filtered and washed with alcohol and deionized water until chloride ions (Cl^-) were no longer detected. The SiO_2 nanoparticles were then chemically modified using chlorotrimethylsilane (CTMS). The white product and 0.05 moles of CTMS were dissolved in 200 milliliters of alcohol, and the solution was heated to 80˚C in a water bath and stirred for 3 hours. After the reaction, the product was filtered and dried under vacuum at room temperature for 24 hours, yielding a powder of SiO_2 nanoparticles with a size range of 40 - 50 nanometers.

Three different modules have been prepared to prepare the proposed adobe brick blocks (Figure 3).

The first model (M1): Natural components (60% clay – 20% sand – 10% lime – 5% pottery powder – 5% straw) that were traditionally used in adobe brick production were used without adding any improvements.

The second model (M2): Involved the addition of nano calcium hydroxide ($Ca(OH)_2$) to the soil mixture and other additives, as the following; (45% clay – 20% (1 - 2 mm maximum aggregate dimension of sand) – 10% red bricks powder – 5% straw – 20% nano lime ($Ca(OH)_2$).

The third model (M3): Involved the addition of nano silica (SiO_2) to the soil mixture and other additives, as the following; (45% clay – 20% (1 - 2 mm maximum aggregate dimension of sand) – 10% red bricks powder – 5% straw – 20% nano silica (SiO_2)).

The previous materials were mixed using a mechanical mixer at 5 to 10 min until homogenized (NF P94-100 Standard) and leave for 28 days to complete the fermentation process, the clay were then formed into mud brick blocks using a mold. Subsequently, distilled water was added to the mixture, adjusting the water concentration to 20% to match the soil's natural moisture content. After preparing the mud brick blocks, they were cut into cubes with dimensions of ($4 \times 4 \times 4$ cm^3), then the specimens were evaluated using various scientific techniques.

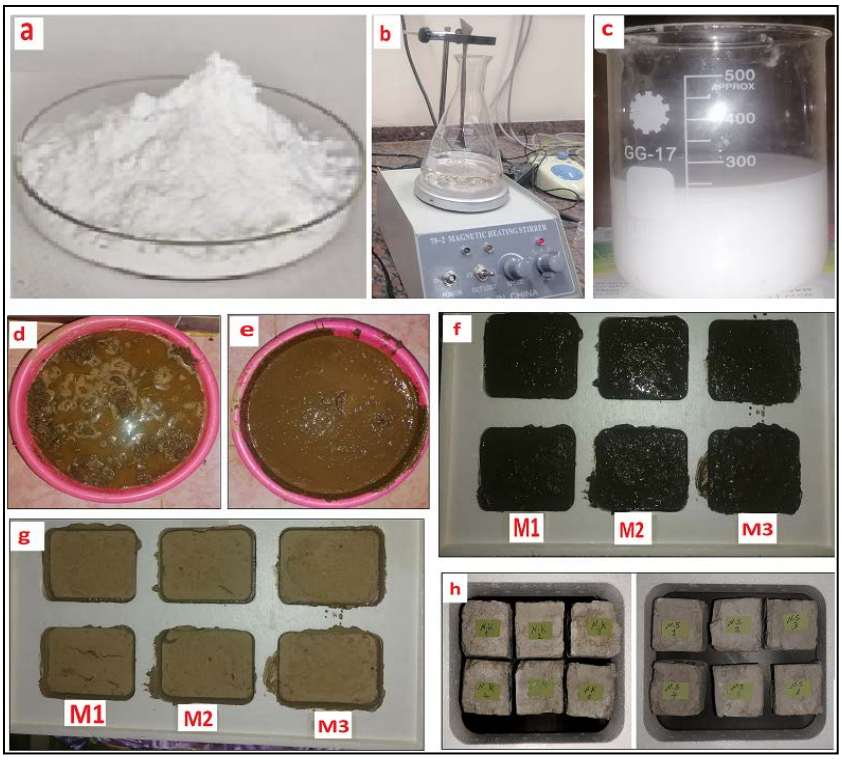

Figure 3. (a) $Ca(OH)_2$ Nanoparticles. (b) (c) SiO_2 nanoparticles. (d) Clay washing stage (this stage is done several times). (e) Clay fermentation stage (leaving for 28 days). (f) The stage of clay forming into blocks of regular dimensions. (g) The mud brick blocks after drying. (h) The mud brick blocks after cut into cubes with dimensions of ($4 \times 4 \times 4$ cm^3).

3.2. The Methods of the Study

3.2.1. Atterberg Limits Test

The Atterberg limits are a set of values that determine the behavior of soil when exposed to moisture. These limits were developed by Swedish scientist Albert Atterberg in the early 20th century. Atterberg limits include three main limits:

- **Liquid Limit (LL):** The limit at which a soil changes from a liquid to a plastic state.
- **Plastic Limit (PL):** The limit at which a soil changes from a plastic to a solid state.
- **Plasticity Index (PI):** It helps determine the behavior of soil when exposed to moisture and is calculated by the difference between the liquid limit and the plastic limit.

Determining Liquid Limit (LL) and plastic limit (PL) experiment (ASTM D4318) (Figure 4):

- The sample is ground and passed through a No. 40 sieve to obtain a homogeneous sample.
- The sample is mixed with a suitable amount of water to obtain a soft paste.
- A portion of the mixture is placed in the front part of the Casagrande device.
- The mixture is divided into two parts using a special tool.
- The device is operated, and the number of blows required for the two parts to close over a distance of (13) mm is recorded.
- Turn on the device, which operates at a rate of two blows per second, causing partial flow of the mixture until the two parts are (13) mm apart. The device is then stopped and the number of blows is recorded.
- After the two parts of the paste have closed, the closed portion is taken and weighed wet, then dried in an oven then weighed dry.
- The test is repeated after changing the water content of the paste, and the number of blows is recorded each time.

The plastic limit (PL) is calculated by the following equation: (**Equation (1)**)

$$\text{Moisture content}\% = (B-C)/(C-A)\times 100 \quad (1)$$

A = Container Weight (g), B = Mass of wet soil + Tare (g), C = Mass of dry soil + Tare (g).

3.2.2. The Physical and Mechanical Properties Test

Physical properties, including bulk density, water absorption, and porosity, were determined in accordance with (ASTM D2487) [22] [23], through laboratory tests using the following equations:

Bulk density: (**Equation (2)**)

$$\rho_{\text{dry}} = M(\text{solid})/V(\text{total}) \quad (2)$$

where ρ = density, M = mass, and V = volume.

Apparent porosity: (**Equation (3)**)

$$n = V(\text{pore space})/V(\text{total}) \tag{3}$$

Capillary Water Absorption: (**Equation (4)**)

$$\text{Water Absorption} = \frac{W_2 - W_1}{W_1} \times 100 \tag{4}$$

where (W_1) dry weight, (W_2) wet weight.

Compressive strength tests were conducted on the specimens in accordance with ASTM 4546-03 [24] [25], and the compressive strength was calculated as follows: (**Equation (5)**)

$$C = F/A \tag{5}$$

where (C) compressive strength of the specimen, (F) total load at which failure occurs in kg, (A) calculated area of the bearing surface in cm^2.

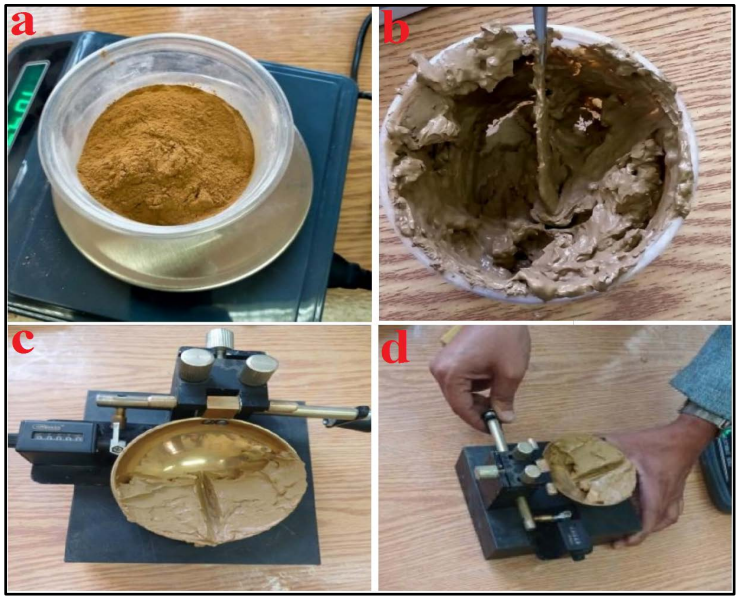

Figure 4. Steps for performing the Atterberg limit test. (a) Weight of the dry soil. (b) The sample is mixed with a suitable amount of water. (c) A portion of the mixture is placed in the front part of the casagrande device. (d) Turn on the device, which operates at a rate of two blows per second.

3.2.3. Examination and Mineralogical Composition

The deteriorated and new mud brick specimens were examined using an Olympus BX40 optical stereo microscope with digital camera recording at 40 - 60 × magnification.

Polarized Light Microscopy (PLM) using a LEITZ WETZLAR (Germany) microscope with a LEICA Cam Max. 100 W camera was utilized to examination thin sections of degraded mud bricks at Faculty of Science at Cairo University, Egypt. The investigation aimed to identify the mineral composition, including mineral types and crystal structures, of the samples. X-ray diffraction (XRD) analysis was performed using a Philips PW 1840 diffractometer with Cu-Kα radiation at 40 kV

and 40 mA. The XRD patterns were collected over a 2θ range of 5˚ to 50˚, providing insights into the mineralogical composition of the mud brick samples. This analysis enabled the identification of mineral phases, and the assessment of weathering induced mineralogical changes.

The microstructure of deteriorated mud brick and improved mud brick specimens were examined before and after 10 cycles of artificial aging using a Quanta 250 Field Emission Gun (FEG) Scanning Electron Microscope (SEM) equipped with an Energy Dispersive X-ray Spectroscopy (EDS) system. The SEM was operated at an accelerating voltage of 30 kV with a magnification range of 30× to 300,000×. The samples were coated with a thin layer using a K550X Sputter Coater (UK) to enhance imaging.

4. Artificial Ageing Cycles

Salt crystallization tests were conducted following the standard method outlined in TS EN 12370 to assess resistance to salt crystallization in mud brick. In order to simulate the effects of salt weathering on the mud brick used in Dendera Temple's adobe enclosure, two types of sodium sulfate (Na_2SO_4) and sodium chloride (NaCl) were used for the ageing testing.

A salt weathering test was carried out on three categories of mud bricks (M1, M2, and M3) to evaluate the resistance of each category to artificial ageing by salt weathering cycles according to the preparation conditions and materials used in each category. 6 adobe cubes were selected for each test.

The specimens were dried in oven at 60˚C for 24 hours, allowing the samples to cool to room temperature and their weights were recorded. Then partially immersed in a 25% solution of sodium chloride (NaCl)/sodium sulfate (Na_2SO_4) for 4 hours, the specimens were dried at room temperature for 8 hours. The specimens were dried in oven at 60˚C for 4 hours, Then repeat these steps for 15 cycles (Figure 5).

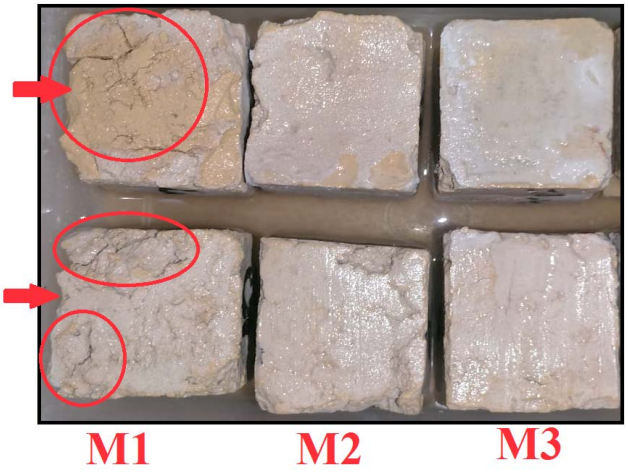

Figure 5. The new mud brick specimens during partial immersion in salt solution, M1 show swelling and cracks in mud brick surface, and M2 and M3 show accumulation of salt on bricks surface.

5. Results and Discussion

5.1. Evaluation of Ancient Mud Brick

The evaluation methodology was according to three criteria as follows: 1) evaluation of physical and mechanical properties, 2) identification of compounds through analysis with X-ray diffraction device, and 3) examination with stereomicroscope, polarizing microscope and examination of the internal structure using scanning electron microscope.

5.1.1. Results of the Physical and Mechanical Properties of Monumental Mud Brick

Evaluation of the physical and mechanical properties of building materials, especially clay bricks, provides an indication of the current condition of the building material and what has happened to it as a result of the influence of various deteriorating factors.

Table 1 shows the physico-mechanical properties which revealed that the Dry density of 1.6 g/cm^2, porosity of 39.5%, water absorption of 29.7% and the compressive strength of ancient mud brick was 1.53 Mpa. Previous results were taken into consideration while preparing the new mud brick.

Table 1. The values of physical and mechanical properties of ancient mud bricks.

Specimens/Tests	Dry density (gr/cm^3)	Porosity (%)	Water absorption (%)	Compressive strength (MPa)
Ancient mud brick	1.6	39.5	29.7	1.53

5.1.2. Examination and Mineralogical Composition of Ancient Mud Brick

Polarized light microscopy (PLM) examination of the mud brick used in the enclosure wall of Dendera Temple revealed a primarily consisting of quartz grains that are medium to coarse-grained, clay minerals including kaolinite, montmorillonite, feldspar minerals comprising albite, gypsum and sodium chloride. Notably, the mud brick exhibited relatively height percentage of clay minerals and salts. clay minerals and salts, as the high percentage of clay minerals caused the swelling phenomenon, which is considered a major cause of damage to adobe blocks.

X-ray diffraction (XRD) analysis of the mud brick samples revealed that they are primarily composed of Quartz (SiO_2) (35%), Kaolinite ($Al_2Si_2O_5(OH)_4$) (23% - 25%), Montmorillonite ($(Na, Ca)0.33(Al, Mg)_2(Si_4O_{10})(OH)_2{\cdot}nH_2O$) (17% - 22%), Albite ($NaAlSi_3O_8$) (7% - 12%), Gypsum ($CaSO_4{\cdot}2H_2O$) (6%), and Halite (NaCl) (5 - 6), as shown in Figure 6.

The deteriorated mud brick was seen by stereomicroscope, exhibiting surface roughening, relief, granular disintegration, and deposits of crystallized salt. SEM investigation verified the presence of internal micro cracks, disintegration of the quartz crystal, loss of binding material, and swelling of clay minerals. In addition to the presence of salts within the internal structure of the brick, this led to the disintegration and tearing of the mineral crystals due to the pressure of crystallization, as shown in Figure 7.

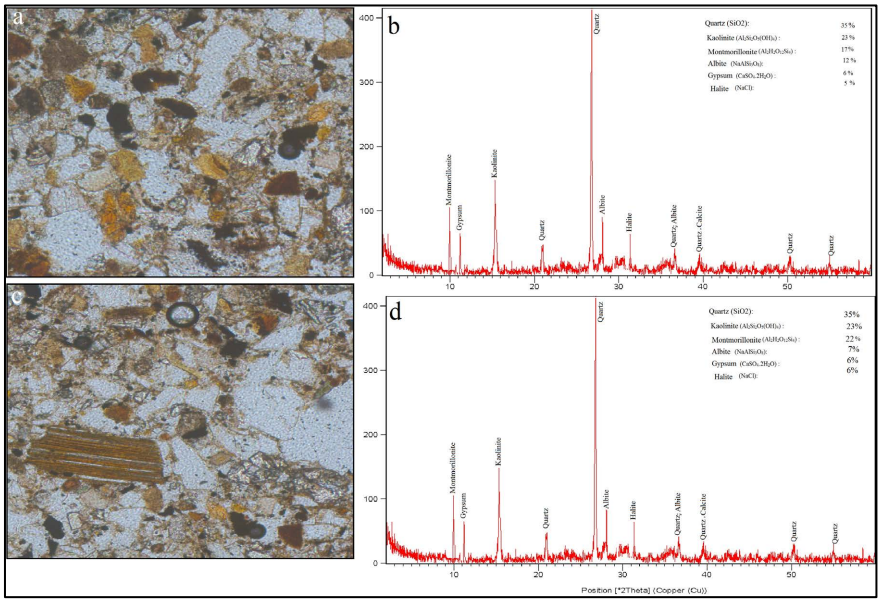

Figure 6. (a) (c) Photomicrograph of thin section of deteriorated mud brick shows quartz grains that are medium to coarse-grained, clay minerals, salts were found. (b) (d) XRD pattern of deteriorated sandstone samples of case study.

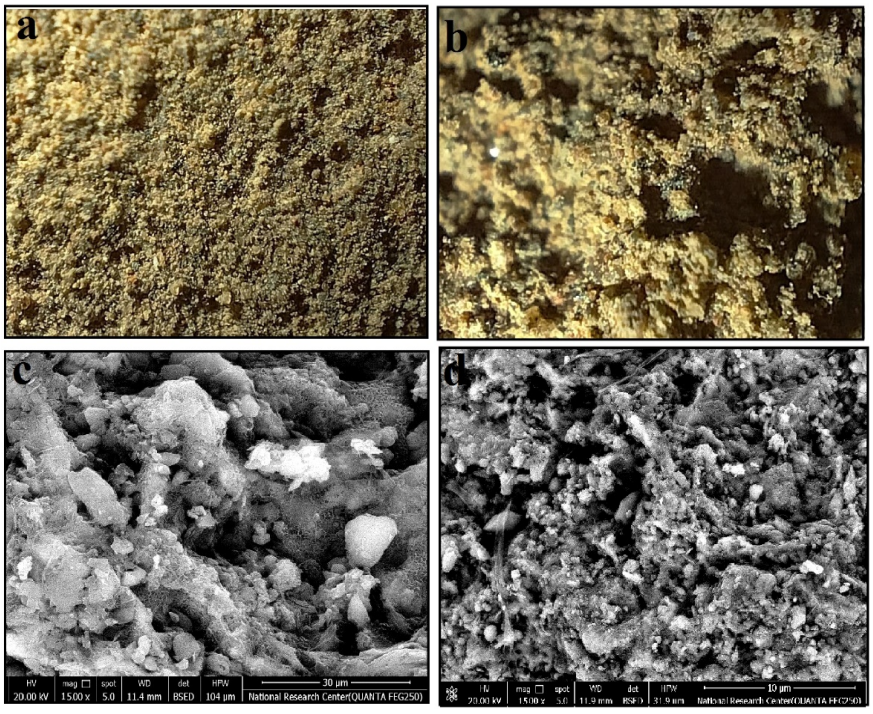

Figure 7. (a) (c) Representative Stereo photomicrograph, exhibiting granular disintegration and the swelling phenomenon. (b) (d) SEM photomicrograph shows the microstructure is rich in clay minerals and salts, and there is also a loss in the brick structure.

5.2. Evaluation of New Mud Brick before and after Artificial Ageing

The evaluation methodology was according to three criteria as follows: 1) evaluation of physical and mechanical properties, 2) visual examination, and 3) exami-

nation with stereo microscope, polarizing microscope and examination of the internal structure using scanning electron microscope.

5.2.1. Results of the Physical and Mechanical Properties of New Mud Brick

Table 2 shows the mean values of atterberg limits test of the three types of mud brick specimens, where the first model (M1), the second model (M2) and the third model (M3). The results obtained from the atterberg limit test show that liquid limit (LL) of the second model (M2) of treated mud brick blocks with calcium hydroxide nanoparticles was 34.2%, a 39.3% decrease compared to the first model of untreated mud brick blocks, liquid limit (LL) of the third model (M3) of treated mud brick blocks with SO_2 nanoparticles was 28.7%, a 49.02% decrease compared to the first model of untreated mud brick blocks.

The results obtained from plastic limit test (PL) of the second model (M2) of treated mud brick blocks with calcium hydroxide nanoparticles was 27% a 40.65% decrease compared to the first model of untreated mud brick blocks. Plastic limit test (PL) of the third model (M3) of treated mud brick blocks with SO_2 nanoparticles was 26%, a 42.85% decrease compared to the first model of untreated mud brick blocks.

Table 2. The mean values of Atterberg limits test of the mud brick specimens.

Atterberg limits test		Liquid Limit (LL)			Plastic Limit (PL)			Plasticity Index (PI)		
	Specimens	M1	M2	M3						
	No of Blows	15	22	29						
	Container No.	C1	C2	C3	M1	M2	M3	M1	M2	M3
A	Container Weight (g)	14	14	14	14	14	14	10.8	7.2	2.7
B	Mass of wet soil + Tare (g)	39	39.2	39.5	30	29.2	30.4			
C	Mass of dry soil + Tare (g)	30	33	33.8	25	26	27			
Moisture content % (B − C)/(C − A) × 100		56.3	34.2	28.7	45.5	27	26			

Figure 8 shows the physico-mechanical properties which revealed that the second model (M2) had an average density of 1.84 g/cm^2, which was a 6.4% increase compared to the density of the first untreated model (M1), which was 1.73 g/cm^2. The third model (M3) achieved an average of 1.85 g/cm^2, an increase of 6.5% compared to the first untreated model (M1).

It was found through a water absorption test that the second model (M2) achieved an average of capillarity water absorption of 6.81%, a decrease of 63.6% compared to the first untreated model (M1), which achieved a water absorption of 18.7%. The third model, M3, achieved an average of capillarity water absorption of 5.89%, a decrease of 68.5% compared to the first untreated model (M1).

It was found through a water absorption test that the second model (M2) achieved an average porosity of 10.35%, a decrease of 63.6% compared to the first untreated model (M1), which achieved a porosity of 28.4%, and the third model

(M3) achieved an average porosity of 9.95%, a decrease of 65% compared to the first untreated model (M1).

The mechanical properties of the mud brick specimens revealed that the second model (M2) had an average compressive strengths (3.6) MPa which achieved a 44% increase compared to the first untreated model (M1), which was (2.5) MPa. The third model (M3) achieved an average of (3.8) MPa an increase of 52% compared to the first untreated model (M1).

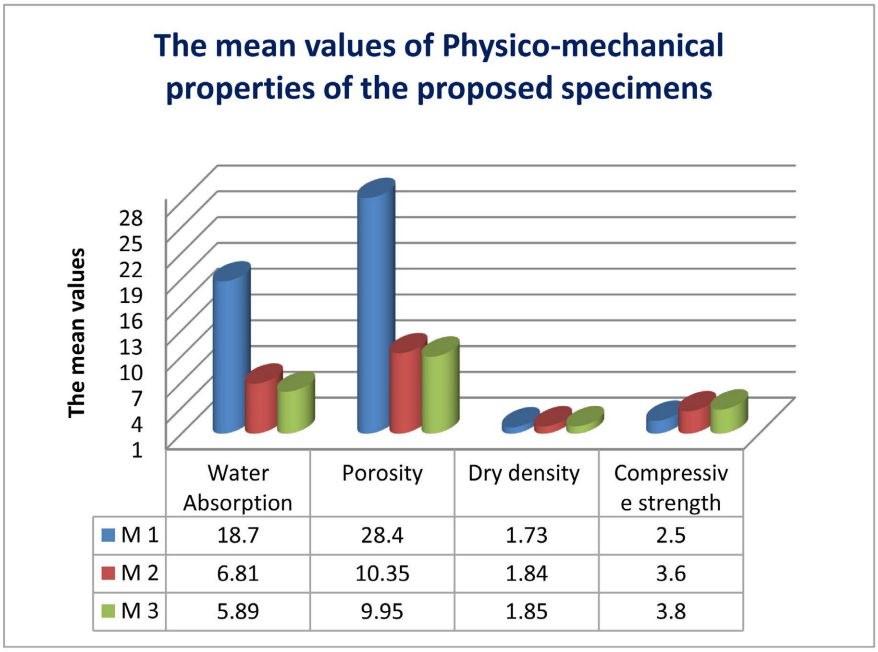

	Water Absorption	Porosity	Dry density	Compressive strength
M 1	18.7	28.4	1.73	2.5
M 2	6.81	10.35	1.84	3.6
M 3	5.89	9.95	1.85	3.8

Figure 8. The mean values of the physico-mechanical properties test of the proposed mud brick specimens.

Figure 9 shows the physico-mechanical properties after artificial ageing by sodium chloride (NaCl)/sodium sulfate (Na_2SO_4). When the mud brick specimens were exposed to salt weathering cycles, it was found that the density of the untreated specimens (M1) decreased by 28.1%, the density of the treated specimens (M2) with nano calcium hydroxide decreased by 18.47%, and the density of the treated specimens (M3) with nano silica decreased by 13.51%.

The results of study revealed that the porosity of the mud brick specimens after subjecting them to salt weathering cycles that the porosity of the untreated specimens (M1) increased by 28.1%, the treated specimens with nano calcium hydroxide (M2) increased by 17.9%, and the porosity of the treated specimens with nano silica (M3) increased by 12.71%.

It was found through a water absorption test that the untreated specimens (M1) increased by 33.9%, the treated specimens with nano calcium hydroxide (M2) increased by 21.7%, and the treated samples with nano silica (M3) increased by 19.31%.

The mechanical properties of the mud brick specimens after artificial ageing

cycles revealed that untreated specimens (M1) had a decrease in compressive strength of 52%, the treated specimens with nano calcium hydroxide (M2) decrease by 25% and the treated samples with nano silica (M3) decrease by 23.7%.

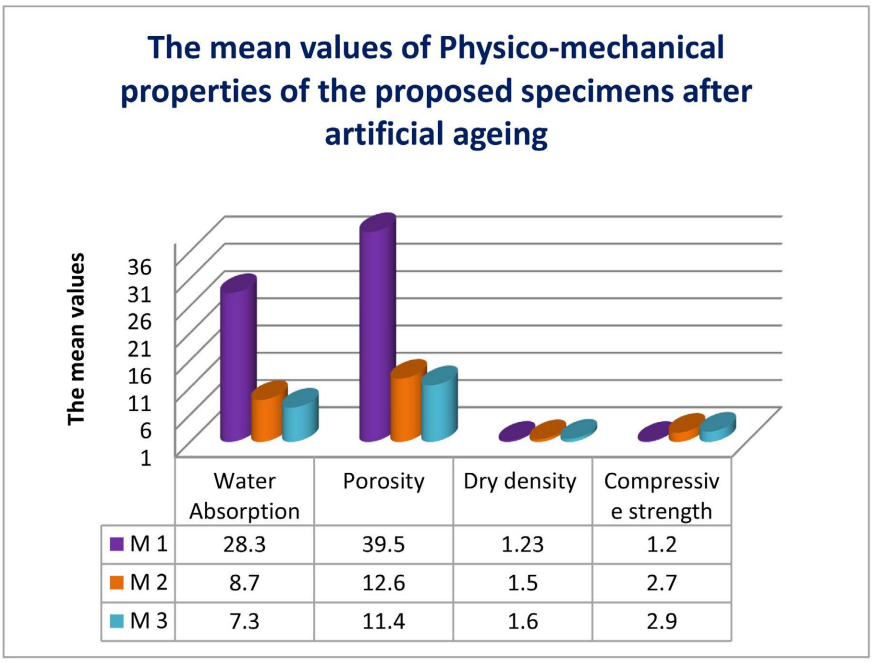

Figure 9. The mean values of the physico-mechanical properties test of the proposed mud brick specimens after artificial ageing cycles.

5.2.2. Examination of New Mud Brick before and after Artificial Ageing

Through visual investigation revealed that the untreated specimens had undergone swelling, effloresce and cracks after 5 cycles and began to corrosion and partially collapse significantly after 10 cycles. As for specimens (M2) and (M3), they showed an accumulation of salt crystals on the surface of the bricks, with slight corrosion appearing after 10 cycles.

Stereomicroscope revealed that untreated mud brick specimens (M1) showed fine grains with low granular disintegration in some places, the treated specimens with nano calcium hydroxide (M2) showed surface homogeneity of fine grains, and the treated specimens with nano silica (M3) showed greater surface homogeneity and grain cohesion than the previous specimens. After the specimens were exposed to salt weathering, stereomicroscope examination revealed that the untreated specimens had undergone significant swelling and the presence of cracks and granular disintegration, in contrast, the treated specimens (M1, M2) had slight erosion but were not swollen by salt weathering as happened in the untreated specimens. SEM microscope revealed that untreated mud brick specimens (M1) showed corrosion of the internal structure of the brick and crystallization of salts with the appearance of swelling of clay minerals, M2 and M3 specimens show a good cohesion of the grains with a slight presence of salt crystals within the brick structure, but without corrosion or gaps (Figures 10-12).

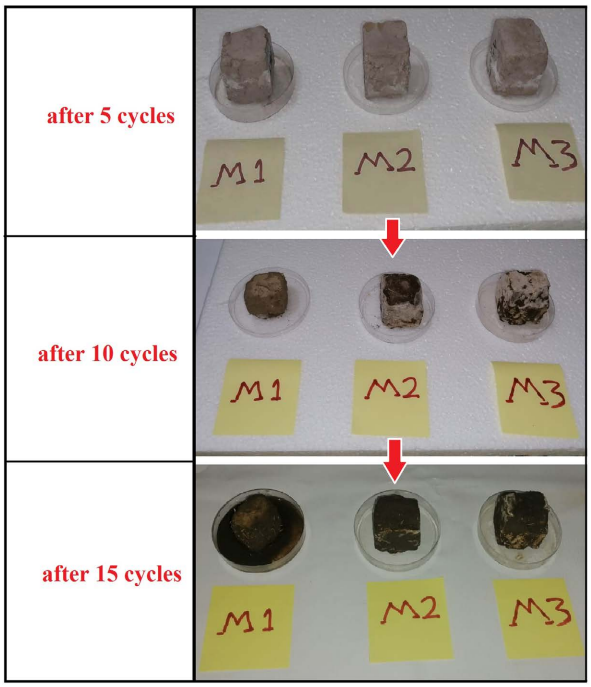

Figure 10. Visual investigation of new mud brick after being subjected to accelerated salts crystallization cycles.

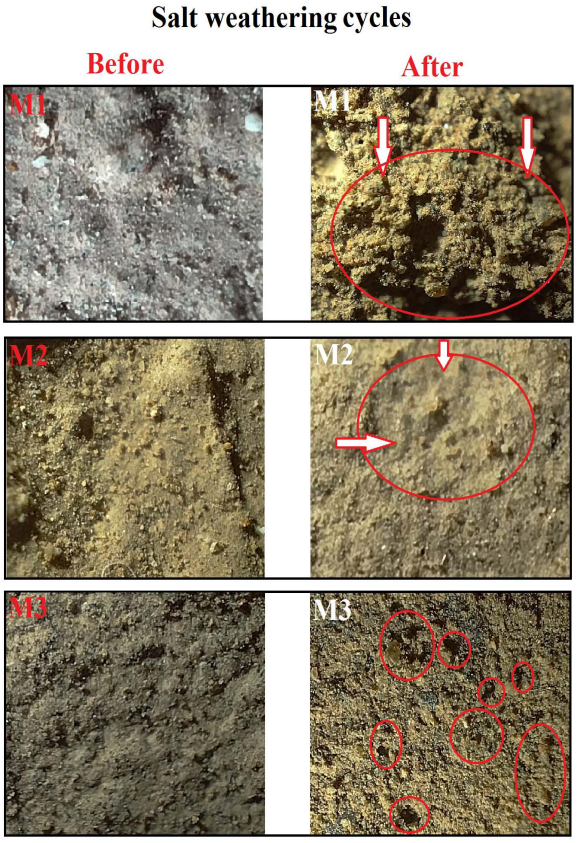

Figure 11. Micrograph show the new mud brick after being subjected to accelerated salts crystallization cycles.

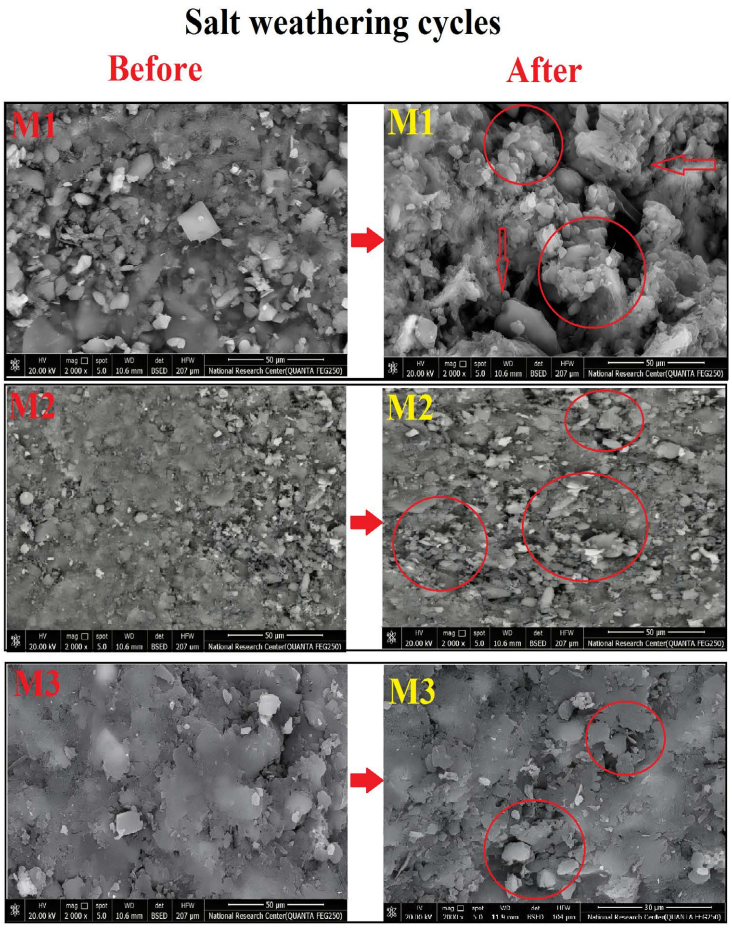

Figure 12. SEM micrograph shows of new mud brick specimens before and after being subjected to accelerated salts crystallization cycles.

6. Conclusions

This study aims to conduct experimental tests to evaluate the durability of nanomaterial-enhanced mud bricks using an accelerated salt weathering test, with the aim of identifying the new mud bricks that are most effective in resisting salt weathering for use in the restoration of the adobe enclosure of Dendera Temple. This study aims to conduct experimental tests to evaluate the durability of enhanced mud brick with nanomaterial using an accelerated salt weathering test. The goal is to identify the new mud brick most effective in resisting salt weathering for use in the restoration of the adobe enclosure of the Dendera temple. After subjecting the new mud bricks to (15) cycles of the salt crystallization test (Na_2SO_4 - NaCl), the specimens were evaluated by the atterberg Limits test (liquid limit (LL), plastic limit (PL), plasticity index (PI)), their physical and mechanical properties, as well as by visual inspection, stereomicroscopy, and scanning electron microscopy (SEM).

Results of the study revealed that adding nanomaterial ($Ca(OH)_2$ - SiO_2) reduced the activity of clay minerals to interact with water contaminate with salt, as

the treated specimens with Nano lime recorded a plasticity rate of 27%, with a decrease rate of 40.65% compared to the untreated specimens, and achieved a resistance rate to swelling pressure of (3.6) MPa. The treated specimens with Nano silica recorded a plasticity rate of 26%, with a decrease rate of 42.85% compared to the untreated specimens, and achieved a resistance rate to swelling pressure of (3.8) MPa.

The results of porosity test of mud brick specimens after subjecting them to salt weathering cycles that the porosity of the untreated specimens (M1) increased by 28.1%, compared to the untreated specimens before artificial ageing, the treated specimens with nano calcium hydroxide (M2) increased by 17.9%, and the porosity of the treated samples with nano silica (M3) increased by 12.71%.

The results of a water absorption test revealed that the untreated specimens (M1) increased by 33.9 %, compared to the untreated specimens before artificial ageing, the treated specimens with nano calcium hydroxide (M2) increased by 21.7%, and the treated specimens with nano silica (M3) increased by 19.31%.

The mechanical properties of the new mud brick specimens after artificial ageing cycles revealed that the untreated specimens (M1) had a decrease in compressive strength of 52 %, the treated specimens with nano calcium hydroxide (M2) decrease by 25 % and the treated samples with nano silica (M3) decrease by 23.7%.

When the specimens were subjected to examination by a stereoscopic and scanning electron microscope, show that there was slight erosion in the internal structure of the treated mud brick specimens with nanomaterial, which was confirmed by the results of the physical properties, with an increase in porosity and water absorption rate as a result of this loss in the internal structure of the specimens. It was also found that the enhanced mud brick specimens with nano-silica were more resistant to salt weathering cycles, and they had a slight decrease in physical and mechanical properties compared to the untreated samples, due to the silicon particles' ability to produce siloxane linkages (Si-O-Si) through hydrolysis, condensation, and polymerization enables them to restore the inter-granular cohesiveness in clay. This process works by reacting with moisture to create hydrolysis, which then turns into a strong "gel" that has similar properties to the natural silicate minerals in mud brick.

In conclusion, the results study revealed that the nanomaterial worked to reduce the activity of clay minerals due to their ability to interact with water molecules, which led to the cessation of the swelling phenomenon and the occurrence of a resistance to swelling pressure ranging from 3.6 to 3.8 MP, with an increase rate of 44% to 52% compared to the untreated specimens.

The study recommends the use of the improved mud bricks (M1 and M2) in the restoration of the adobe enclosure of Dendera Temple, and the use of nanomaterial ($Ca(OH)_2$ - SiO_2) for consolidation of ancient mud brick.

Conflicts of Interest

The author declares no conflicts of interest regarding the publication of this paper.

References

[1] Debowska-Ludwin, J. (2020) "Another Brick in the Wall" or How to Build an Ancient Egyptian House. *Archaeological Review from Cambridge*, **25**, 57-73.

[2] Buchez, N., Gerez, J., Guérin, S. and Minotti, M. (2021) The Emergence of Mudbrick Architecture in Egypt in the 4th Millennium BCE. Reflection Based on Recent Discoveries at Tell El-Iswid (Eastern Delta). *Archéo-Nil. Revue de la société pour l'étude des cultures prépharaoniques de la vallée du Nil*, **31**, 111-134. https://doi.org/10.3406/arnil.2021.1360

[3] Iyer, N.L. (2014). Performance Evaluation of Clay Grout Formulations for Structural Cracking in Historic Earthen (Mud Brick) Buildings. Master's Thesis, University of Pennsylvania. https://repository.upenn.edu/handle/20.500.14332/37106

[4] Hershey, R., Kalina, M., Kafodya, I. and Tilley, E. (2023) A Sustainable Alternative to Traditional Building Materials: Assessing Stabilised Soil Blocks for Performance and Cost in Malawi. *International Journal of Sustainable Engineering*, **16**, 155-165. https://doi.org/10.1080/19397038.2023.2237062

[5] Rainer, L. (2008) Deterioration and Pathology of Earthen Architecture. *Terra Literature Review*, **45**, 1-174.

[6] Cooke, L. (2008) Approaches to the Conservation and Management of Earthen Architecture in Archaeological Contexts. Master's Thesis, University of London.

[7] Du, J. (2023) Swelling Mechanism and Swelling Behaviour of Expansive Clay and Clay Minerals. Master's Thesis, RMIT University.

[8] Barrera, J.M. (2024) Dendera, Temple of Time: The Celestial Wisdom of Ancient Egypt. Simon and Schuster.

[9] Kumari, N. and Mohan, C. (2021) Basics of Clay Minerals and Their Characteristic Properties. In: Do Nascimento, G.M., Ed., *Clay and Clay Minerals*, IntechOpen. https://doi.org/10.5772/intechopen.97672

[10] Michalopoulou, A., Maravelaki, N.P., Stefanis, N.A., Theoulakis, P., Andreou, S., Kilikogloul, V. and Karatasios, I. (2020) Evaluation of Nanolime Dispersions for the Protection of Archaeological Clay-Based Building Materials. *Mediterranean Archaeology and Archaeometry*, **20**, 221-242.

[11] Tariq, L.R. and Jafaar, A.M. (2024) A Review of Nanotechnology in Self-Healing of Ancient and Heritage Buildings: Heritage Buildings, Nanomaterial, Nano Architecture, Nanotechnology in Construction. *International Journal of Nanoelectronics and Materials* (*IJNeaM*), **17**, 153-163. https://doi.org/10.58915/ijneam.v17i1.602

[12] Prudêncio, M.I., Stanojev Pereira, M.A., Marques, J.G., Dias, M.I., Esteves, L., Burbidge, C.I., *et al.* (2012) Neutron Tomography for the Assessment of Consolidant Impregnation Efficiency in Portuguese Glazed Tiles (16th and 18th Centuries). *Journal of Archaeological Science*, **39**, 964-969. https://doi.org/10.1016/j.jas.2011.11.010

[13] García-Vera, V.E., Tenza-Abril, A.J., Solak, A.M. and Lanzón, M. (2020) Calcium Hydroxide Nanoparticles Coatings Applied on Cultural Heritage Materials: Their Influence on Physical Characteristics of Earthen Plasters. *Applied Surface Science*, **504**, Article ID: 144195. https://doi.org/10.1016/j.apsusc.2019.144195

[14] Venkatarama Reddy, B.V. and Latha, M.S. (2014) Retrieving Clay Minerals from Stabilised Soil Compacts. *Applied Clay Science*, **101**, 362-368. https://doi.org/10.1016/j.clay.2014.08.027

[15] Harrou, A., Lechheb, M., El Ouahabi, M., Fagel, N. and Gharibi, E. (2024) Physicochemical Properties and Microstructure of Bentonite in Highly Alkaline Environments. *Clays and Clay Minerals*, **72**, e15. https://doi.org/10.1017/cmn.2024.27

[16] Franzoni, E., Pigino, B., Leemann, A. and Lura, P. (2013) Use of TEOS for Fired-Clay Bricks Consolidation. *Materials and Structures*, **47**, 1175-1184. https://doi.org/10.1617/s11527-013-0120-7

[17] Barrera, J.M. (2024) Dendera, Temple of Time: The Celestial Wisdom of Ancient Egypt. Simon and Schuster.

[18] Wilkinson, R.H. (2005) Die Welt der Tempel im alten Ägypten. Theiss.

[19] El-Gohary, M. (2012) The Contrivance of New Mud Bricks for Restoring and Preserving the EDFA Ancient Granary-Sohag, Egypt. *International Journal of Conservation Science*, **3**, 67-78.

[20] El-hafez, M.A. (2018) Characterization and Restoration Recommendations of Some Adobe Shrines at El-Bagawat Cemetery, Kharga Oasis, Western Desert-Egypt. *Egyptian Journal of Archaeological & Restoration Studies*, **8**, 1-13.

[21] Mohamed, E.H. (2025) An Experimental Study on Consolidated Sandstone by Accelerated Salt Crystallization Cycles: A Case Study of Dendera Temple, Qena, Egypt. *Research on Engineering Structures and Materials*, **11**, 985-1002. https://doi.org/10.17515/resm2025-804st0406rs

[22] Illampas, R., Ioannou, I. and Charmpis, D.C. (2009) Adobe: An Environmentally Friendly Construction Material. *WIT Transactions on Ecology and the Environment*, **120**, 245-256. https://doi.org/10.2495/sdp090241

[23] Mohamed, E.H. (2023) Effectiveness Assessment of Paraloid B-72 Enhanced with Nano Materials to Improve of Completion Mortars Properties for Conservation of Seti I Temple in El-Qurna, Thebes West Bank, Egypt. *Multiscale and Multidisciplinary Modeling, Experiments and Design*, **6**, 371-387. https://doi.org/10.1007/s41939-023-00152-1

[24] ASTM Standard (2011) D2487-11 Standard Practice for Classification of Soils for Engineering Purposes (Unified Soil Classification System). ASTM International.

[25] Mebarki, M., Benyahia, S. and Dahmani, S. (2025) Laboratory Improvement of Clay Mineralogical and Swelling Properties Using Hydraulic Binder Treatment. *Research on Engineering Structures and Materials*, **11**, 933-955. https://doi.org/10.17515/resm2025-752ma0313rs